

Mapping planted forests in the Korean Peninsula using artificial intelligence








Ankita Mitra, César Iván Álvarez, Akane O. Abbasi, Nancy L. Harris, Guofan Shao, Bryan C. Pijanowski, Mohammad Reza Jahanshahi, Javier G. P. Gamarra, Hyun-Seok Kim, Tae-Kyung Kim, Daun Ryu, Jingjing Liang

Angaben zur Veröffentlichung / Publication details:

Mitra, Ankita, César Iván Álvarez, Akane O. Abbasi, Nancy L. Harris, Guofan Shao, Bryan C. Pijanowski, Mohammad Reza Jahanshahi, et al. 2024. "Mapping planted forests in the Korean Peninsula using artificial intelligence." *Forests* 15 (7): 1216. <https://doi.org/10.3390/f15071216>.

Article

Mapping Planted Forests in the Korean Peninsula Using Artificial Intelligence

Ankita Mitra ¹, Cesar Ivan Alvarez ², Akane O. Abbasi ¹, Nancy L. Harris ³, Guofan Shao ⁴, Bryan C. Pijanowski ^{4,5}, Mohammad Reza Jahanshahi ^{6,7}, Javier G. P. Gamarra ⁸, Hyun-Seok Kim ^{9,10,11}, Tae-Kyung Kim ⁹, Daun Ryu ^{11,12} and Jingjing Liang ^{1,*}

- ¹ Forest Advanced Computing and Artificial Intelligence (FACAI) Lab, Department of Forestry and Natural Resources, Purdue University, 715 Mitch Daniels Blvd., West Lafayette, IN 47907, USA; mitra46@purdue.edu (A.M.); akane.abbasi@gmail.com (A.O.A.)
 - ² Environmental Research Group for Sustainable Development (GIADES), Salesian Polytechnic University, Rumichaca y Moran Valverde, Quito 170702, Ecuador; calvarezm@ups.edu.ec
 - ³ World Resources Institute, 10 G Street N.E., Washington, DC 20002, USA; nancy.harris@wri.org
 - ⁴ Department of Forestry and Natural Resources, Purdue University, 715 Mitch Daniels Blvd., West Lafayette, IN 47907, USA; shao@purdue.edu (G.S.); bpijanow@purdue.edu (B.C.P.)
 - ⁵ Center for Global Soundscapes, Department of Forestry and Natural Resources, Purdue University, 715 Mitch Daniels Blvd., West Lafayette, IN 47907, USA
 - ⁶ Lyles School of Civil and Construction Engineering, Purdue University, 550 Stadium Mall Drive, West Lafayette, IN 47907, USA; jahansha@purdue.edu
 - ⁷ Elmore Family School of Electrical and Computer Engineering, Purdue University, 610 Purdue Mall, West Lafayette, IN 47907, USA
 - ⁸ Forest Monitoring and Data Platforms (FMDP) Team, Forestry Division, Food and Agriculture Organization of the United Nations, Viale delle Terme di Caracalla, 00153 Rome, Italy; javier.garciaperez@fao.org
 - ⁹ Department of Agriculture, Forestry, and Bioresources, Seoul National University, Seoul 08826, Republic of Korea; cameroncrazies@snu.ac.kr (H.-S.K.); bmkim88@snu.ac.kr (T.-K.K.)
 - ¹⁰ Research Institute of Agriculture and Life Sciences, Seoul National University, Seoul 08826, Republic of Korea
 - ¹¹ Interdisciplinary Program in Agricultural and Forest Meteorology, Seoul National University, Seoul 08826, Republic of Korea; aldoi0314@gmail.com
 - ¹² Livable Urban Forests Research Center, National Institute of Forest Science, Seoul 02455, Republic of Korea
- * Correspondence: albeca.liang@gmail.com



Citation: Mitra, A.; Alvarez, C.I.; Abbasi, A.O.; Harris, N.L.; Shao, G.; Pijanowski, B.C.; Jahanshahi, M.R.; Gamarra, J.G.P.; Kim, H.-S.; Kim, T.-K.; et al. Mapping Planted Forests in the Korean Peninsula Using Artificial Intelligence. *Forests* **2024**, *15*, 1216. <https://doi.org/10.3390/f15071216>

Academic Editor: Yihang Zhang

Received: 31 May 2024

Revised: 3 July 2024

Accepted: 9 July 2024

Published: 12 July 2024



Copyright: © 2024 by the authors. Licensee MDPI, Basel, Switzerland. This article is an open access article distributed under the terms and conditions of the Creative Commons Attribution (CC BY) license (<https://creativecommons.org/licenses/by/4.0/>).

Abstract: Forests are essential for maintaining the ecological balance of the planet and providing critical ecosystem services. Amidst an increasing rate of global forest loss due to various natural and anthropogenic factors, many countries are committed to battling forest loss by planting new forests. Despite the reported national statistics on the land area in plantations, accurately delineating boundaries of planted forests with remotely sensed data remains a great challenge. In this study, we explored several deep learning approaches based on Convolutional Neural Networks (CNNs) for mapping the extent of planted forests in the Korean Peninsula. Our methodology involved data preprocessing, the application of data augmentation techniques, and rigorous model training, with performance assessed using various evaluation metrics. To ensure robust performance and accuracy, we validated the model's predictions across the Korean Peninsula. Our analysis showed that the integration of the Near Infrared band from 10 m Sentinel-2 remote sensing images with the UNet deep learning model, incorporated with unfrozen ResNet-34 backbone architecture, produced the best model performance. With a recall of 64% and precision of 76.8%, the UNet model surpassed the other pixel-based deep learning models, including DeepLab and Pyramid Sense Parsing, in terms of classification accuracy. When compared to the ensemble-based Random Forest (RF) machine learning model, the RF approach demonstrates a significantly lower recall rate of 55.2% and greater precision of 92%. These findings highlight the unique strength of deep learning and machine learning approaches for mapping planted forests in diverse geographical regions on Earth.

Keywords: planted forests; artificial intelligence; climate change; remote sensing

1. Introduction

Forests, encompassing 31% of the world's land area [1], are essential ecosystems that provide numerous environmental, social, and economic benefits, but the world is losing forest cover at an alarming rate. These ecosystems are vital in mitigating climate change by sequestering and storing carbon [2–4]. Additionally, forests contribute to soil conservation, stabilize water flow, and prevent land degradation and natural disasters. Forests hold immense cultural, aesthetic, and recreational value while also playing a significant role in poverty alleviation and economic development by providing essential resources such as food, timber, and various forest products [1]. Due to deforestation and forest degradation, the world lost 437,000 km² of tree cover between 2010 and 2022 ([5]; <https://www.globalforestwatch.org/> (accessed on 15 November 2023)). This deforestation and extensive forest degradation significantly impact global ecosystem functioning, climate change mitigation efforts, and biodiversity conservation. Forest degradation, exacerbated by climate change, also includes damage caused by pests such as beetles. These pests pose a serious threat to forest health, leading to increased tree mortality and further degradation. Studies have utilized multispectral imaging to classify tree species and assess their health status, effectively detecting healthy, unhealthy, and dead trees affected by bark beetle infestations [6]. Early detection and management of forest health issues are crucial, providing valuable insights for conservation and forest management efforts. It is therefore essential to monitor and assess the impacts of such degradation using advanced remote sensing data to address the challenges posed by forest pests and climate change [7–11].

Planted forests are deliberately established through artificial tree planting or seeding, and they play a crucial role in generating income, providing goods, and addressing climate change while restoring ecosystem services and processes [12]. The global implementation of active tree planting for climate change mitigation, forest restoration, and biological conservation highlights the urgent need to formulate cost-effective guidelines for both ongoing and future tree-planting projects [13]. Assessment of the costs and benefits of planted forests, the key to the development of such cost-effective guidelines, is contingent on knowing where the existing planted forests are distributed [14] and which tree species are planted [9]. While national governments have published some planted forest maps utilizing in situ forest records and satellite data, there remains a pressing need for comprehensive and cost-effective guidelines to guide tree-planting initiatives on a global scale [15].

The Republic of Korea (ROK, also known as South Korea) is internationally recognized for its successful restoration of healthy forests after World War II and the Korean War, due to a series of planting efforts by the government [16,17]. Yet, the spatial coverage of the national data records remains unverified for the rest of the Korean Peninsula. Our knowledge of the exact locations of planted forests is limited, partly because (1) the decentralized responsibility for establishing and managing planted forests involving private entities, individual landowners, and small-scale enterprises often results in less formal reporting and data collection than in larger forested areas under state ownership [18], (2) the spatial distribution of planted forests across different jurisdictions creates complexities in implementing standardized monitoring systems, further impeding comprehensive data collection [19], and (3) historical research focus on natural forests has led to limited attention and resources allocated to documenting these man-made ecosystems [19]. The lack of consistent documentation hampers precise assessments of the extent, condition, and biodiversity of planted forests, which are vital for understanding their critical roles in carbon sequestration, biodiversity conservation, and sustainable resource management [20]. Without this information, it becomes challenging to make informed decisions that maximize the ecological, economic, and social benefits of these forests. Thus, a map that provides a complete projection of the geographic distribution of planted forests in the Republic of Korea is not just a step towards creating a consistent and harmonized product but also a vital tool in guiding effective environmental policy and forest management strategies. Failure to address this gap could lead to continued mismanagement, resulting in impaired

ecosystem services and diminished carbon storage capacity, undermining efforts to combat climate change and preserve natural resources.

Convolutional Neural Networks (CNNs) utilized in semantic segmentation have revolutionized computer vision and object detection in recent years, including for remote sensing data analysis [21–25]. Past studies have demonstrated the potential of CNNs in forestry applications, achieving high accuracy in classifying tree species from hyperspectral imagery [26–28] and grouping forest types from other remote sensing images such as Sentinel-2 imagery [29,30]. These studies, along with others [31,32], have shown that diverse machine learning approaches, particularly those incorporating CNNs, possess the capability to discern pertinent patterns within these data recordings.

Advances in artificial intelligence algorithms [33], particularly deep learning techniques, have opened new possibilities in identifying planted forests. Deep learning (DL) algorithms can extract complex features from satellite data and accurately classify different types of land cover, including forests, over large geographical areas. These approaches have also been applied to semantic segmentation tasks, which involve labeling each pixel in an image with a corresponding class label, such as forest or non-forest [34]. The UNet model, for instance, has demonstrated superior performance in segmenting forest areas from aerial imagery compared to traditional machine learning methods [28] as well as in medical science in detecting diseases [35–38]. Similarly, studies using DeepLab for delineating forest boundaries from remote sensing data have shown the model’s capability to capture fine details and improve the accuracy of forest maps [39]. These advancements in deep learning and pattern recognition have paved the way for more accurate and efficient analysis of satellite imagery, facilitating the mapping of complex features in forestry applications on a large scale.

Moreover, there is significant potential in leveraging remote sensing data for forest monitoring, given its high temporal resolution and widespread availability, often at no cost, as is the case with Copernicus Sentinel-2 imagery [40]. In addition to neural networks, ensemble machine learning models such as Random Forest (RF), incorporating Sentinel-2 images, have been extensively used in forestry studies [41–44]. These studies, including those on land cover classification, demonstrate the robustness and high accuracy of RF models in handling complex datasets [45]. However, traditional machine learning techniques, while effective, often rely solely on spectral information and may not capture the intricate patterns and spatial relationships present in the data as effectively as deep learning models [22]. Thus, the advancements in deep learning and CNNs in pattern recognition have significantly enhanced the ability to discern relevant patterns within remote sensing data, offering unprecedented opportunities for accurate mapping and monitoring of forests [46]. These developments highlight the potential of leveraging remote sensing data and advanced artificial intelligence models to address the challenges of forest management and conservation effectively.

In this study, we aim to map the extent of planted forests across the Korean Peninsula by integrating advanced deep learning methodologies with space-based, multispectral remote sensing data. The ground truth data, essential for training and validation, consisted of South Korea’s in situ government records of forest cover from 2020. This dataset included a polygon map delineating planted forests. From this map, we created a response variable with explicit labels distinguishing “planted” from “natural” forests. Our primary objective was to compare the performance of various deep learning architectures—UNet, DeepLab, and the Pyramid Scene Parsing Network (PSPNet)—to determine the most effective model for recognizing planted forests within the designated training area on Jeju Island. Our secondary objective was to examine the accuracy and efficacy of various deep learning and ensemble-based machine learning model approaches. The most effective model, as determined by this comparative analysis, was subsequently utilized to project the extent of planted forests across the entire peninsula. This study leverages high-resolution satellite imagery, thus enabling improved mapping of planted forested areas, thereby contributing significantly to the fields of ecological monitoring and land use management.

2. Materials and Methods

We utilized satellite imagery as the background layer to classify planted forests within the Korean Peninsula. The imagery was acquired using different bands from two platforms, Landsat-8 and Sentinel-2, which allowed us to capture comprehensive information about the land cover. To ensure accuracy and efficacy, we compared the performance of these platforms. Our study involved the application of three pixel-based deep learning models for an extensive classification of planted forests. This approach further facilitated the generation of a high-resolution map of about 10 m illustrating the spatial distribution of planted forests across the Republic of Korean Peninsula (RoK). To bolster the robustness of our approach, we initially integrated a rigorous K-fold cross-validation technique [47], a critical component that enhances the credibility and generalizability of our research findings. This systematic validation process confirms the reliability and applicability of our results in mapping the planted forests within our study region. Following this, we further validated our model across the Korean Peninsula to ensure its efficiency and effectiveness for applications and mapping on larger geographic scales.

2.1. Study Area

We conducted a comprehensive deep learning analysis on Jeju Island of the Korean Peninsula (Figure 1), utilizing satellite images of the year 2020. Jeju Island, located in the Republic of Korea and spanning an area of 1842 km² with a population of 697,349 as of 2021, is characterized by volcanic origins and divided into three distinct regions based on altitude: the coast (0–200 m), mid-mountain (200–600 m), and mountainous areas (>600 m) [48]. Recognized for its exceptional natural beauty, Jeju Island holds prestigious UNESCO designations, including Biosphere Reserve (2002), World Natural Heritage Site (2007), and Global Geopark (2010) [49]. Additionally, the island features two intangible UNESCO cultural heritages and a world agricultural heritage site, emphasizing its significance in terms of ecosystem preservation, cultural heritage, and tourism resources. Over the past 50 years, Jeju Island has experienced significant land use changes [50]. Despite its acclaim, the island faces threats to biodiversity, including invasive exotic species and a notable loss of natural habitat and quality due to land development associated with increased tourism [48]. Thus, Jeju Island serves as a representative study area for the entire Korean Peninsula due to its diverse ecosystems, UNESCO-recognized heritage, and the impact of land use changes [50], providing insights applicable to broader environmental contexts and sustainable practices in forest management.

Our methodology comprised two main steps: a geospatial approach and a deep learning approach. In the geospatial approach, we compiled government-based in situ planted forest observations of 2020, and integrated them with extensive remote sensing imagery, allowing for a thorough geospatial mapping of planted forest regions. Subsequently, in the deep learning approach, we employed three different pixel-based deep learning models to train and analyze the compiled data. This synergetic approach, combining geospatial and deep learning methodologies utilizing ground truth data and remote sensing images, enabled a robust and comprehensive mapping of planted forest areas. To achieve this, we employed a four-stage process, as illustrated in Figure 2. In Stage 1, we acquired Sentinel-2 images at a 10 m resolution [51] from the summer and fall of 2020 using the Google Earth Engine (GEE) [52] for background imagery. These satellite imageries were merged to create a composite image overlaid with ground-truth data of planted forests from Jeju Island. We then applied comprehensive data cleaning and augmentation processes to ensure accuracy and reliability in our analysis. Firstly, we mapped the satellite data to ensure accurate alignment and consistency with the geographic coordinates of the ground-truth data. This involved overlaying the Sentinel-2 imagery with the ground-truth data to visually inspect and verify spatial congruence. Using ArcGIS 3.0.3, we matched the spatial extent of the imagery with the expected locations of planted forests, ensuring each data point corresponded accurately to its real-world position. Secondly, we conducted an outlier analysis by comparing the observed data points with the expected patterns of

planted forests. Outliers were identified as data points that significantly deviated from the expected spatial distribution and were flagged using visual inspection [53]. To improve image quality, we incorporated the s2cloudless machine learning algorithm in the Google Earth Engine (GEE) [54,55] and further used data augmentation techniques to expand the training dataset [56–58]. These steps ensured that our dataset was clean, accurate, and reliable for subsequent analysis stages, enhancing the overall robustness of our study. Next, manual labeling was performed to identify and classify planted forests, and the processed and labeled data were exported for model training and testing. In Stage 2, we trained the UNet model [59] using different backbone architectures [60], including ResNet 18 and ResNet 34, with hyperparameter tuning [61] to determine the optimal settings. Stage 3 involved assessing the performance of the UNet model using various evaluation metrics and comparing it to other pixel-based deep learning models and the Random Forest ensemble machine learning model [62]. Based on the evaluation results, the UNet model with ResNet 34 backbone architecture was selected as the best-performing model for our mapping. Finally, in Stage 4, we used the optimized UNet model to project and map the extent of planted forests across the entire peninsula.

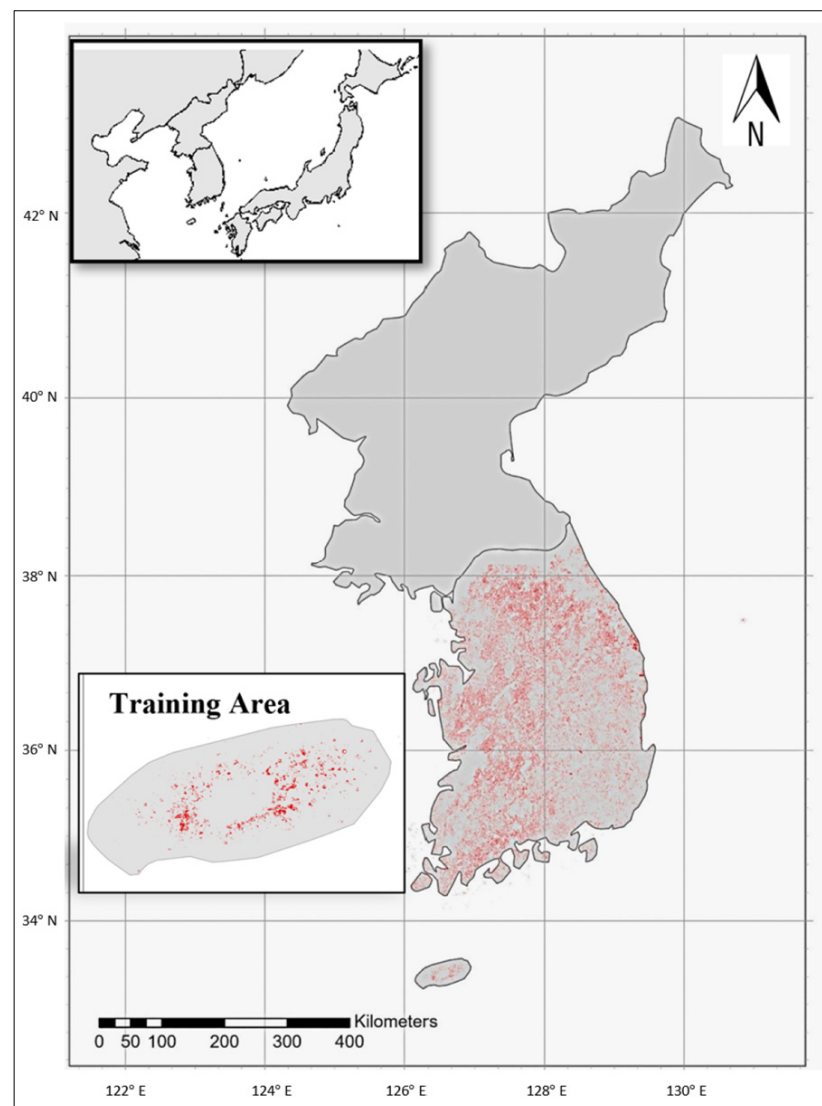


Figure 1. The study region—the Korean Peninsula consists of the Republic of Korea (ROK) and the Democratic People's Republic of Korea (DPRK). Jeju Island in the south of ROK was used in this study as the training area (inset box) where the red areas represent the ground-truth planted forest data obtained from the national government records.

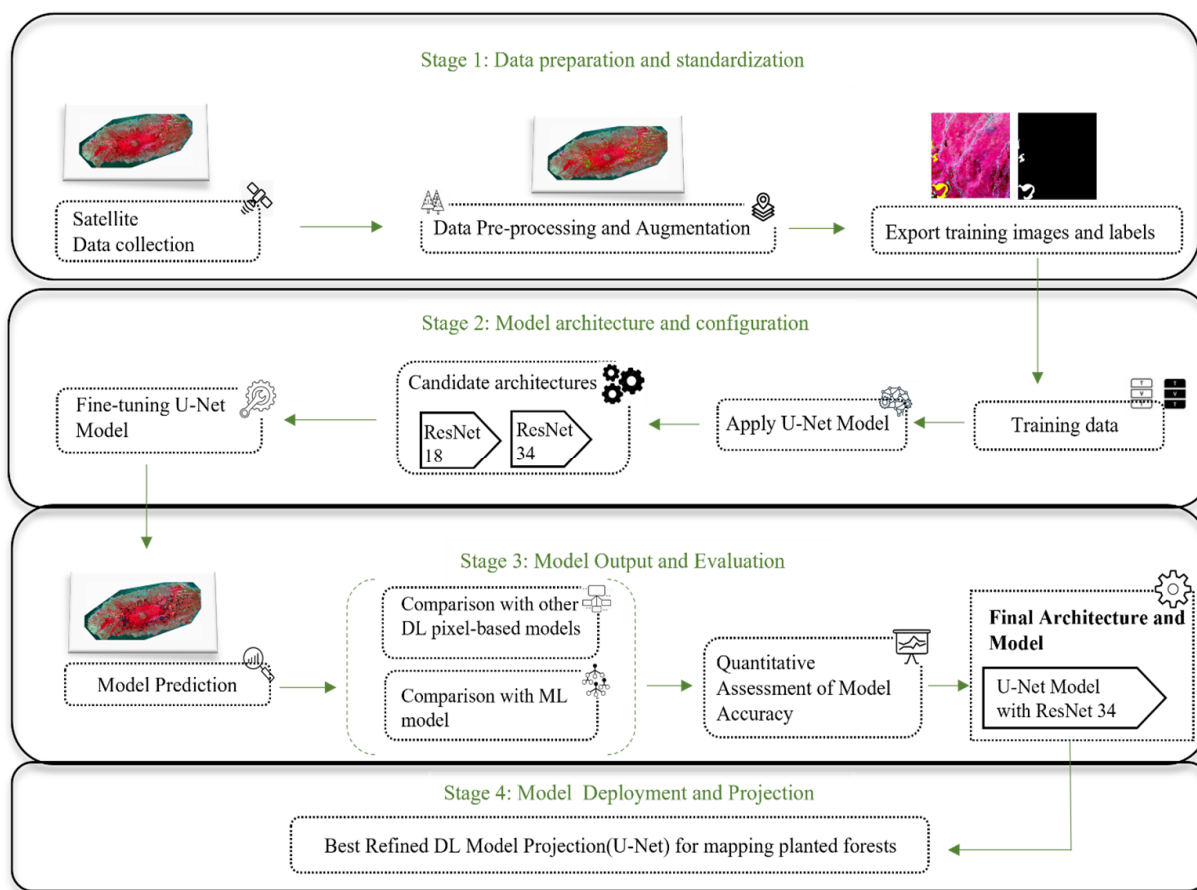


Figure 2. A conceptual diagram of the four-stage process employed in the study. Stage 1 involved data acquisition and preprocessing; Stage 2 focused on model training and hyperparameter tuning; Stage 3 involved model evaluation and selection; and Stage 4 projected the mapped forests across the Korean Peninsula.

2.2. Data Acquisition and Fusion

We initiated our data collection process by compiling the in situ forest cover data from South Korea’s national government records for 2020. To complement this, we acquired satellite imagery tiles from the same year using GEE. This temporal alignment is crucial as it ensures consistency and accuracy in the datasets, eliminates discrepancies that could arise from using data from different time periods, and allows the model to reflect contemporary conditions of planted forests, accounting for recent changes and dynamics in the ecosystem. It also enhances the model’s training process by enabling it to learn true relationships and patterns from temporally aligned data, providing a robust foundation for accurately assessing the model’s performance and ensuring reliable validation results. The satellite images featured distinct band combinations and resolutions, allowing for a comprehensive detection of the planted forest areas. We meticulously explored combinations of Red, Green, Blue, and Near-InfraRed spectral bands—specifically B4, B3, and B2 (Red-Green-Blue bands) and B8, B4, and B3 (NIR-Red-Green bands)—with varying resolutions from Landsat-8 (30 m) and Sentinel-2 (10 m) data to identify the optimal sensor performance and configuration for our deep learning model in improved prediction of the planted forests. Our initial findings highlighted that those imageries acquired during mid-summer to early fall provided the clearest and brightest results as compared to the other seasons. We subsequently conducted data pre-processing techniques to remove the outliers as well as the additional noise and atmospheric interferences such as cloud cover, smog, and canopy shadows.

Our input data for the model training purpose thus comprised the collected ground truth record for planted forests coupled with processed background satellite imagery from both Landsat-8 and Sentinel-2 of the year 2020. To further enhance the robustness of our training dataset and mitigate model overfitting, we implemented a variety of data augmentation techniques, including random rotation, scaling, and flipping [57,58,63]. By diversifying the training data, the augmentation process enabled the model to effectively capture and discern patterns from various angles and orientations, thereby enhancing its learning capacity and predictive accuracy. Through this process, we generated a total of 1640 training samples, each comprising tiles sized at 256×256 with minimal overlap. The resulting training data, enriched through meticulous data augmentation hence served as a foundation for training a robust and generalized deep learning model. Following this, we randomly divided the training samples into two sets, allocating 80% for training and 20% for validation. Additionally, we reserved an independent dataset from the Korean Peninsula to further evaluate our model's efficiency in prediction. This approach allowed us to rigorously test and validate the model's performance across different datasets, ensuring its robustness and generalizability. Leveraging the unique spectral characteristics and spatial resolutions of both sensors, we utilized the ground truth data to accurately label and classify the planted forests within the study area. We utilized the Export Training Data for the Deep Learning tool in ArcGIS Pro 3.0.3 to facilitate the extraction of training samples for the model training purpose. Each training sample comprised image tiles paired with corresponding binary labels, where pixel values were represented as 0 for non-planted forests and 1 for planted forests. Subsequently, we proceeded to train the UNet deep learning model to identify the regions of planted forests. UNet is widely recognized for its effectiveness in image segmentation tasks and is adept at capturing contextual information while maintaining spatial resolution [59].

2.3. Model Training

We trained the UNet model for the semantic segmentation of planted forest classes using remote sensing imagery of Jeju Island. This model comprises a contracting and expanding path and is designed for pixel-wise classification of input images. The UNet architecture follows an Encoder–Decoder approach, where the encoder utilizes a pre-trained CNN such as ResNet, and the decoder restores the original dimensions of the image [59]. The contracting path employs a recurring pattern involving a pair of successive 3×3 convolutions, each followed by a rectified linear unit (ReLU) activation, in addition to a 2×2 max pooling operation with a stride of 2 for efficient down-sampling. This progressive down-sampling operation contributes to a two-fold increase in the number of feature channels at each step [64]. Conversely, the expansive path is characterized by a procedure of feature map up-sampling, succeeded by a 2×2 convolution, often referred to as “up-convolution”, which effectively reduces the number of feature channels by half [65]. The output of this up-convolution operation is concatenated with a suitably cropped version of the corresponding feature map from the contracting path. This concatenated result undergoes 2 consecutive 3×3 convolutions with ReLU activation to further refine the feature representation. The requirement for cropping arises because of the border pixel loss incurred during each convolutional operation. The architectural finality is realized by means of a 1×1 convolutional layer, positioned as the ultimate stage. This layer undertakes the task of mapping each 64-component feature vector to the desired number of classes, effectively yielding the segmentation outcome [66]. Cumulatively, the UNet model is structured with a cumulative total of 23 convolutional layers. The contracting path excels at capturing contextual and high-level features, while the expansive path facilitates the localization of intricate details. The recurring reliance on 3×3 convolutions is meticulously considered. This particular kernel size is chosen due to its adeptness in striking a balance between capturing fine-grained local information and recognizing more comprehensive, global patterns within the data [67]. For a brief outline of technical concepts in deep learning, please refer to Box 1.

We conducted a comprehensive evaluation of pixel-based semantic segmentation models for the classification of planted forests from non-planted forests. We additionally explored two backbone architectures, namely ResNet 18 and ResNet 34, to assess the performance of the UNet model prediction. While more complex backbone configurations, such as Efficient-net-b0 to Efficient-net-b7, have shown the potential for improved results [68–71], we considered the significant computational costs associated with them as a major drawback. Therefore, in our study, we opted for ResNets, which balance computational efficiency and performance. ResNets achieve this by introducing cardinality, allowing for reduced computational costs while maintaining satisfactory results [72]. To further ensure a thorough analysis, we compared the model performance of UNet with the other state-of-the-art pixel-based classification models, namely DeepLab [73] and Pyramid Scene Parsing (PSP) [74]. An overview of the architecture for each of the models used in this study is outlined in the Supplementary Section (Box S1).

Box 1. Technical concepts in deep learning.

- Semantic Segmentation: This process involves assigning a specific label to every pixel in an image, enabling the distinction between different objects or land cover classes within the scene.
- Convolutional Neural Networks (CNNs): Specialized deep neural networks widely used in analyzing visual imagery. They utilize convolution operations to process data with grid-like topology, such as images.
- ReLU (Rectified Linear Unit): An activation function that introduces non-linearity in the network, essential for learning complex patterns.
- Max Pooling: A technique that reduces the spatial dimensions of an input feature map, making the network invariant to small translations and helping in feature detection.
- Up-convolution (Transposed Convolution): Used to increase the spatial dimensions of an input feature map, commonly in tasks requiring precise localization, such as image segmentation.

The training process covered the entire area of Jeju Island (Figure 1), and we utilized the Training Deep Learning model tool in ArcGIS Pro for this purpose. For the training phase, we randomly selected 80% of image pairs from the overall dataset. We adopted a batch-based approach, where the entire dataset was not required to be prepared and pushed into the GPU for training simultaneously [63]. Instead, the data of each batch were processed sequentially, allowing training to commence in parallel with the preparation of the remaining data. This approach conferred the advantage of initiating training promptly without the necessity of preparing and storing the entire dataset beforehand. Moreover, the processed data could be directly streamed into the Graphics Processing Unit (GPU) without the intermediate step of storage on the hard disk. This streamlined process enhanced efficiency and resource utilization during the model's training. Throughout the training phase, we monitored loss curves and employed various performance metrics for evaluation, ensuring a comprehensive assessment of model performance. To optimize the performance of our deep learning models and address the class imbalance, we opted for the dice loss function as our selected loss function [75]. Moreover, we thoroughly adjusted hyperparameters [61], such as the number of epochs, batch sizes, freezing, and unfreezing the weights of the background model architecture (ResNets). These refinements played a crucial role in optimizing the model's performance for the detection of the planted forests. After this fine-tuning process and the integration of these optimizations, we successfully projected the most refined deep learning model to have an improved understanding of the coverage of planted forest regions across the entire Korean Peninsula (Figure 3). Additionally, we demonstrated how this approach effectively identifies planted forests across different ecoregions within the peninsula (Figure 4), showcasing the method's capability to accurately capture the diverse ecological characteristics of the area.

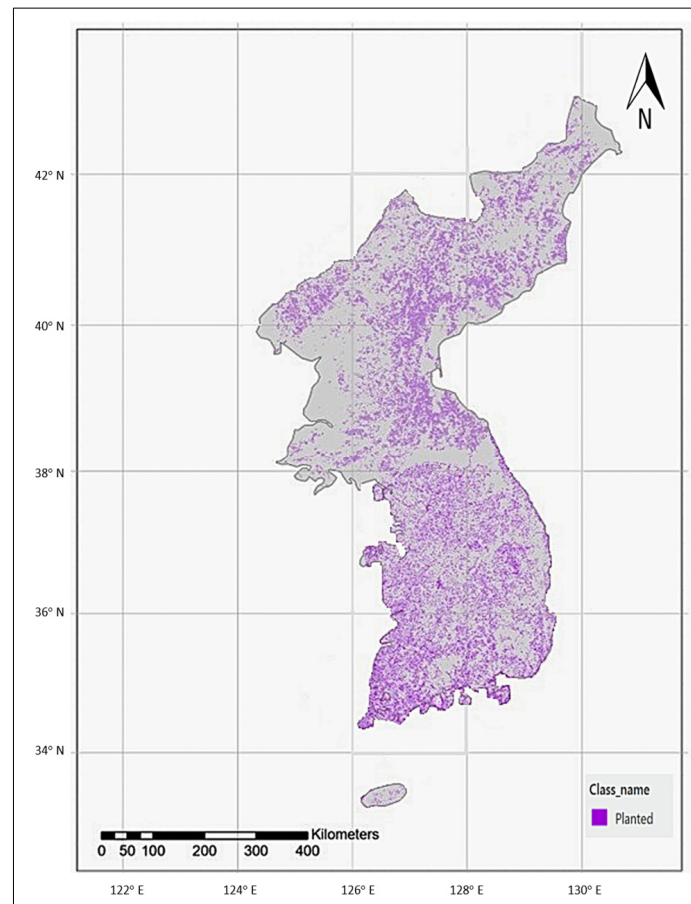


Figure 3. Projected planted forest locations on the Korean Peninsula in 2020. The projection was made with a UNet deep learning model, based on 10 m resolution Sentinel-2 satellite imagery.

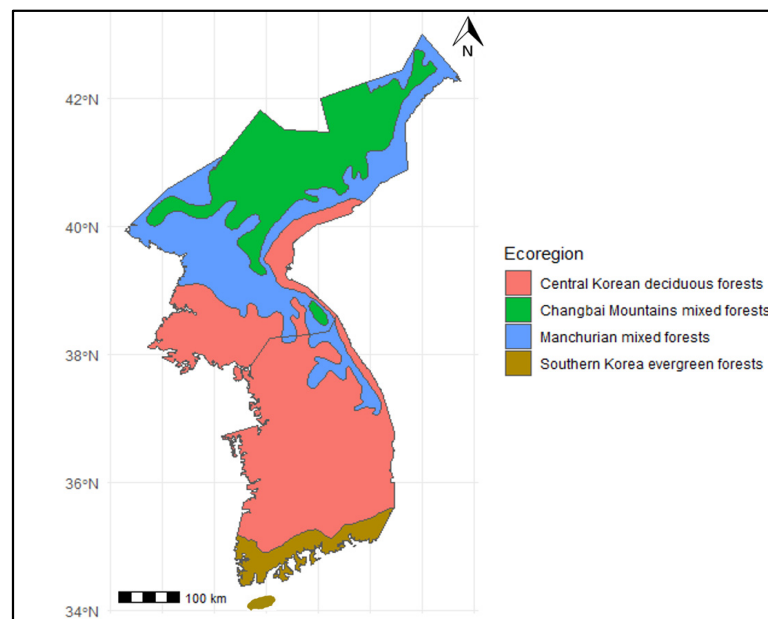


Figure 4. WWF terrestrial ecoregions of North and South Korea. The map illustrates the distribution of different ecoregions: Central Korean deciduous forests, Changbai Mountains mixed forests, Manchurian mixed forests, and Southern Korea evergreen forests.

2.4. Model Evaluation

To conduct a comprehensive evaluation of the deep learning model's segmentation accuracy, we computed the Intersection over Union (IoU) score, a crucial metric in assessing the accuracy of the deep learning approach [76]. This analysis focused specifically on the two-band combinations, aiming to offer valuable insights for the optimal selection of bands in our study. IoU scores for B4, B3, and B2, and B8, B4, and B3 from the 10 m Sentinel 2 satellite were computed using GPU resources on Google Collab. The score gauges the overlap between predicted and actual segmentation masks, commonly used in semantic segmentation tasks, with a higher IoU score indicating improved segmentation performance.

Another important aspect of evaluating a deep learning model's performance is analyzing the loss curve, which also provides insights into the model's performance [77]. The loss curve shows the trend of the model's training and validation loss over the number of epochs or batches processed. This provides insights into how well the model learned from the training data and how well it generalizes to new data. A well-fitting loss curve decreases over the epochs and stabilizes at a point without overfitting or underfitting [77,78]. Therefore, the loss curve analysis is significant in determining if the model has learned efficiently from the training data and if it can perform well on new data.

Additionally, we compared the top-performing deep learning model from this study with the conventional Random Forest (RF) machine learning model, which has been widely used in ecological and biological research with satisfactory performance [79,80]. We utilized the "randomForest" package in R [81] to perform the analysis. The RF model was trained by extracting pixel values of the satellite bands, which subsequently served as the predictor variables. The response variable for this model comprised the ground-truth planted forest data of Jeju Island. The methodology adopted for training the RF model mirrored that of the deep learning approach, encompassing an initial K-fold 80:20 cross-validation approach for partitioning training and validation datasets to assess the model performance during the training phase [47,82]. We further validated our model using an independent dataset from across the Korean Peninsula to ensure its robustness and generalizability. By aligning these techniques, we ensured a consistent and equitable evaluation framework.

We analyzed the performance of the models using several accuracy metrics such as precision, recall, and F1 score, each offering valuable insights into the model's effectiveness [83,84]. While accuracy is commonly used and easily understood for evaluating classification problems, it tends to overstate the performance of imbalanced data [85]. A high overall accuracy does not necessarily ensure good performance in all aspects and therefore we need to consider precision, recall, and F1 score for a comprehensive evaluation. Precision (P) assesses the proportion of correctly classified positive predictions among the total predicted positives. Recall (R) measures the proportion of correctly classified positive predictions among the total actual positives [86]. The F1 score, being an equal combination of precision and recall, offers a balanced evaluation perspective of incorrectly predicted cases and thus is a more suitable metric for assessing models dealing with imbalanced datasets [87]. These metrics play a crucial role in our study, considering the potential impact of false positives and false negatives on result interpretation. For instance, a high precision and low recall would suggest that the model correctly identifies positive predictions but may miss some actual positive instances.

3. Results

3.1. Performance Metrics Assessment

The preliminary test indicated that the Near Infrared-Red-Green band (B8, B4, B3) extracted from Sentinel-2 satellite imagery, featuring a 10 m resolution, exhibited superior outcomes in terms of model performance when compared against Landsat 30 m satellite data and the standard RGB bands and NIR-R-G bands (Table 1). As a consequence of these findings, the extraction of the 10 m resolution Near Infrared-Red-Green Band (B8, B4, B3) data from Sentinel-2 satellite imagery was utilized for further analysis. This step subsequently generated training tiles, forming the basis for an encompassing evaluation of

the model's performance across the entire expanse of the Korean Peninsula. Notably, it was observed that the overall model performance was improved when utilizing a training tile of size 256×256 over 512×512 . This adjustment was based on the hypothesis that larger tile dimensions, such as 512×512 , might potentially overlook intricate details, thereby impeding the deep learning model's capacity to learn with precision.

Table 1. Comparison of UNet model evaluation metrics on Jeju Island to evaluate the best background satellite resolution with the band combination, based on ResNet 18 unfrozen backbone architecture.

Background Satellite	Resolution	Band Combinations	Precision	Recall	F1 Score
Sentinel-2	10 m	B4, B3, B2	75.0%	45.4%	56.6%
Sentinel-2	10 m	B8, B4, B3	81.2%	47.8%	60.2%
Landsat-8	30 m	B4, B3, B2	4.2%	2.1%	3.3%
Landsat-8	30 m	B8, B4, B3	4.6%	2.6%	3.5%

We also examined how different augmentation methods affected the model's performance using the best band combination from the Sentinel-2 data, specifically B8, B4, and B3 (Table 2). Without augmentation, the model has a baseline precision of 70.5%, a recall of 30.2%, and an F1 score of 42.3%. Applying random rotation improves recall significantly to 44.2% and the F1 score to 54.8%, while scaling further enhances precision to 74.0% and the F1 score to 56.2%. Flipping maintains a balance with improvements in both precision (73.5%) and recall (43.1%), resulting in an F1 score of 54.3%. The combined augmentation approach yields the highest performance across all metrics, with precision at 76.8%, recall at 64.0%, and an F1 score of 69.8%. This indicates that utilizing multiple augmentation techniques together significantly enhances the model's ability to generalize and perform robustly across various scenarios.

Table 2. Performance metrics for different data augmentation techniques on B8, B4, and B3 band combination of Sentinel-2 10 m.

Augmentation Method	Precision	Recall	F1 Score
No augmentation	70.5%	30.2%	42.3%
Random rotation	72.1%	44.2%	54.8%
Scaling	74.0%	45.3%	56.2%
Flipping	73.5%	43.1%	54.3%
Combined approach	76.8%	64.0%	69.8%

3.1.1. Intersection over Union (IoU) Performance

The resulting IoU scores of the UNet model from two different band combinations (Red-Green-Blue and NIR-Red-Green) were found to be 93% and 95%, respectively (Figure 5). This revealed a strong alignment between predicted and actual ground truth masks. In the early epochs, fluctuations were expected as the model learned to recognize patterns within the data. However, as training progressed, the curve gradually stabilized in later epochs, with a diminishing gap between the training and validation datasets. This trend indicates an improvement in the model's performance over time, with enhanced consistency in its predictions across both sets. Given these insights, we opted to prioritize the B8, B4, and B3 band combination due to its higher Intersection over Union (IoU) score, suggesting superior performance in accurately delineating planted forest areas.

3.1.2. Loss Curve Performance

The analysis of loss curves is another critical step in evaluating the ability of a deep learning model to predict unknown data. In our study, the Training Deep Learning Model tool in ArcGIS Pro was used to generate loss curves and assess the model performance with two different band combinations (B8, B4, B3 vs. B4, B3, B2) of Sentinel-2 satellite data.

The optimal loss curve reflects a well-trained model that strikes a balance between fitting the data and avoiding overfitting or underfitting, suggesting that our model captured the complexities of the training data and can generalize to new data. Our findings revealed a consistent decrease in both training and validation loss as the number of processed batches increased, eventually converging and stabilizing (Figure 6). This indicates that the model effectively learned from the training and validation samples, demonstrating the capability to make accurate predictions on unseen data. Moreover, the band combination of B8, B4, and B3 from Sentinel-2 satellite imagery proved more suitable for our analysis, as evidenced by the better convergence rate of the training and validation curves. This suggests that incorporating the NIR band can capture relevant features more effectively for the prediction task in Jeju Island.

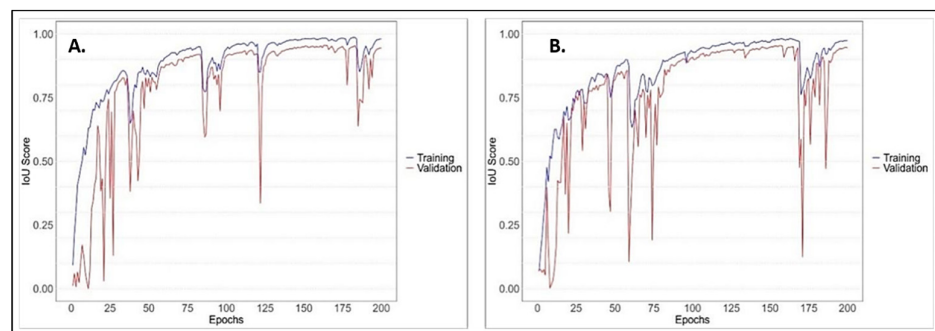


Figure 5. The Intersection over Union (IoU) scores of the proposed UNet model for the training and validation datasets on the Republic of Korean Peninsula, based on (A) Red-Green-Blue Band (B4, B3, B2) and Sentinel-2 10 m resolution background imagery; and (B) Near-InfraRed-Red-Green Band (B8, B4, B3) and Sentinel-2 10 m resolution background imagery.

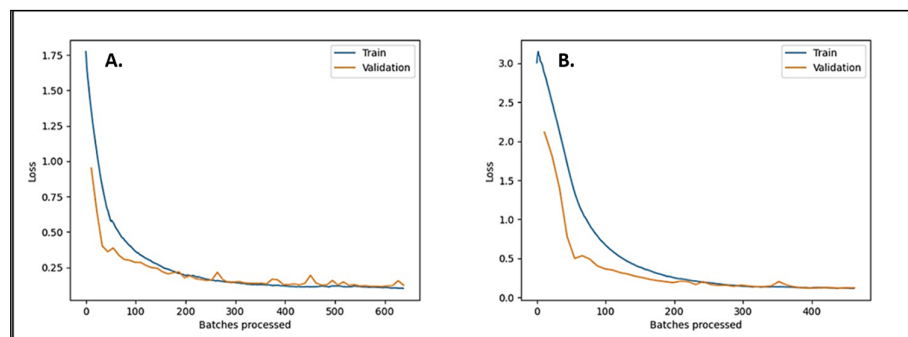


Figure 6. The Loss Curves of the training and validation datasets, estimated with the UNet Model for Republic of Korean Peninsula. The UNet model was trained using (A) Red-Green-Blue Band (B4, B3, B2) and Sentinel-2 10 m resolution background imagery; and (B) Near-InfraRed-Red-Green Band (B8, B4, B3) and Sentinel-2 10 m resolution background imagery.

3.1.3. Classifier's Performance

With the selection of the B8, B4, and B3 bands from Sentinel-2 10 m resolution background imagery confirmed, our focus shifted towards a thorough evaluation of the model's efficacy. This involved integrating additional metrics such as precision, recall, and the F1 score. By incorporating these metrics, we gained a more nuanced understanding of the model's effectiveness, enhancing the depth of our analysis. Notably, the other pixel-based deep learning models, namely DeepLab and Pyramid Scene Parsing, yielded unsatisfactory results in terms of precision, recall, and F1 score, with their loss curves exhibiting instability. Consequently, to optimize computational resources and save time, we opted not to compute IoU scores for these alternative deep learning models.

Table 3 presents a summary of the evaluation metric results involving different hyperparameters for UNet semantic segmentation architectures, which included backbones

like ResNet18 and ResNet34. These variations encompassed hyper tuning of factors such as weight freezing or unfreezing, number of epochs, and batch size. The evaluation revealed that freezing the weights of the ResNet 18 backbone architecture resulted in poor performance compared to the ResNet 34 backbone, with precision, recall, and F1 scores of approximately 78.1%, 44.2%, and 56.4%, respectively. In contrast, unfreezing the weights of the ResNet 34 backbone architecture with 200 epochs yielded the best results, with precision, recall, and F1 scores of 76.8%, 64.0%, and 69.8%, respectively (Figure 7). Specifically, our deep learning model in Jeju achieved a precision value of 76.8%, indicating that 76.8% of the predicted planted forests were correctly identified. The recall value was 64%, indicating that 64% of the actual planted forests were detected by the model. The F1 score, which provides an overall measure of the model’s performance, was 69.8%. Further experimentation with other hyperparameters revealed minimal performance differences in F1 score between the unfrozen weighted ResNet 34 models. However, the unfrozen weighted ResNet 34 model trained for 200 epochs with a batch size of 20 exhibited the highest F1 score. These findings suggest that the UNet model with the ResNet 34 backbone architecture is suitable for mapping planted forests in the Korean Peninsula, as it provides effective performance metrics such as precision, recall, F1 score, and IoU score. Nonetheless, the UNet model with the ResNet 34 backbone framework provided adequate and effective metrics for mapping planted forests in the Korean Peninsula.

Table 3. Evaluation metrics after model parameterization to improve the UNet model accuracy on the Republic of Korean Peninsula, based on the Sentinel-2 10 m (B8, B4, B3) selected.

Background Architecture	Freeze/Unfreeze Weights	Epochs	Batch Size	Precision	Recall	F1 Score
RESNET 18	Freeze	20	8	78.1%	44.2%	56.4%
RESNET 18	Unfreeze	20	8	81.2%	47.8%	60.2%
RESNET 34	Freeze	20	8	73.5%	48.0%	58.1%
RESNET 34	Unfreeze	20	8	76.8%	50.2%	60.0%
RESNET 18	Freeze	200	20	74.3%	9.1%	15.8%
RESNET 18	Unfreeze	200	20	78.1%	40.4%	53.3%
RESNET 34	Freeze	200	20	80.3%	45.5%	58.0%
RESNET 34	Unfreeze	200	20	76.8%	64.0%	69.8%

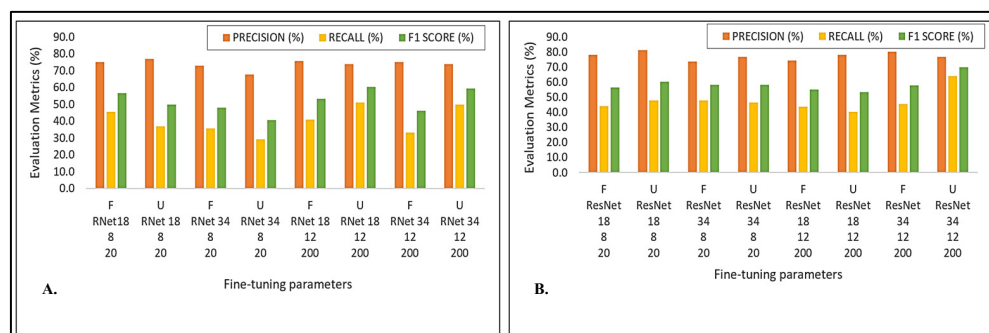


Figure 7. Evaluation metrics of the proposed UNet model of Jeju Island across different backbone architectures and hyperparameters (F-Freezing weights; U-Unfreezing weights; Batch (8; 12) Epochs (20; 200)), and two different band combinations: (A) Red-Green-Blue Band (B4, B3, B2) of Sentinel-2 10 m resolution background imagery; and (B) Near-InfraRed-Red-Green Band (B8, B4, B3) of Sentinel-2 10 m resolution background imagery.

Further comparing the UNet model with the ensemble-based RF model over the Republic of Korea Peninsula, noteworthy distinctions emerged. Table 4 illustrates that the precision, recall, and F1 scores for the RF model were 92%, 55.2%, and 69%, respectively. In comparison, the UNet model exhibited a precision of 76.8%, a recall of 64%, and an F1 score

of 69.8%. In this context, it is evident that the UNet model demonstrated a substantially greater recall rate and a slightly higher F1 score.

Table 4. Comparative Performance Assessment of the different pixel-based deep learning models versus Random Forest machine learning model, based on the selected unfrozen backbone architecture (ResNet 34).

Models	Precision	Recall	F1 Score
UNet	76.8%	64.0%	69.8%
DeepLab	60.8%	32.4%	42.3%
Pyramid Scene Parsing (PSP)	8.9%	51.9%	15.1%
Random Forest (RF)	92.0%	55.2%	69.0%

4. Discussion

Accurately mapping the spatial distribution of planted forests is crucial for promoting sustainable forest management practices and making informed decisions to establish global and national strategies aimed at social, ecological, and economic development [88]. Recent studies employing primarily Landsat images and utilizing non-deep learning methods [89,90], as well as other deep learning approaches [91–93], have demonstrated high performance and the capability to cover extensive areas. However, precisely identifying the locations of planted forests across the Korean Peninsula presents a formidable challenge, given the vast continental size and diverse topographic and climatic conditions of the region. To address these obstacles, remote sensing technology combined with deep learning offers numerous advantages and is an efficient approach for current research [94].

The visual interpretation of color differences between natural and planted forests can be complex and difficult for the human eye. The current study thus utilized a semantic segmentation deep learning approach with three Sentinel-2 channels (NIR-Red-Green), a departure from most CNN studies [27,95–97] that rely solely on RGB channels. The human eye can only see the visible range of the electromagnetic spectrum, which includes red, green, and blue light [98]. Healthy vegetation reflects more green light than other wavelengths, indicating higher chlorophyll content while absorbing more red and blue light [99]. As a result, we perceive healthy forests as green. However, specialized sensors can detect other spectral bands, such as Near Infrared (NIR), which are invisible to the human eye but provide new insights into forest features on Earth [100,101].

Through random visual inspection, we found that most of the categorized planted forests in Korea exhibited an evenly spaced horizontal structure. Studies [102–105] reported that planted trees are mostly arranged in rows in afforestation areas that create canopy gaps, thereby generating heterogeneity in the spectral response, leading to increased reflectance variation. This structured planting pattern resulted in distinct spectral vegetation health signatures, such as the Normalized Difference Vegetation Index (NDVI), and other spectral band values. These were inspected using the Google Earth Engine (GEE) algorithm [106], enabling a detailed analysis of the vegetation health and spatial distribution in planted forests. Thus, integrating deep learning algorithms with remote sensing data [107,108] allows for improved detection of these planted forest patterns, offering significant improvements over traditional methods in terms of accuracy and scalability. In contrast to traditional machine learning techniques, such as Random Forest that rely solely on spectral information without incorporating textual measures, deep learning approaches, on the other hand, have recently emerged as a promising tool for identifying features of interest and achieving state-of-the-art performance [64,109,110].

Our study demonstrated that applying data augmentation techniques significantly enhanced the model's performance. Specifically, rotation improved the model's generalization capabilities, with a slight increase in recall and F1 scores, suggesting enhanced recognition of objects from different orientations. Scaling led to a noticeable improvement in precision, indicating better identification of planted forests with varying sizes. Flipping contributed

to a balanced improvement in both precision and recall, thereby enhancing the overall F1 score. The combined augmentation approach yielded the highest performance metrics across all categories, demonstrating that leveraging multiple augmentations together provides a more comprehensive improvement in the model's generalization capabilities and resilience to different environmental conditions and data anomalies. Furthermore, our study highlighted that integrating the Near Infrared (NIR) band with the UNet deep learning model and an unfrozen ResNet-34 backbone architecture produced the best model performance. Our analysis of the loss curves and comparison of evaluation metrics indicate that our UNet deep learning model, trained on the band combination of B8, B4, and B3 for 10 m Sentinel-2 satellite data, is well suited for predicting planted forests over the entire peninsula and is ready for practical deployment in predicting unknown data. It is worth noting that our study provides valuable insights into the performance comparison of other deep learning pixel-based models for forest mapping applications. Based on the findings, we conclude that among the three pixel-based classification models, UNet is the best choice for our objective of mapping planted forests in the RoK. Its superior performance, stable loss curves, and ability to capture complex patterns and representations make it highly suitable for accurate and reliable forest mapping applications [110,111]. The UNet model effectively leverages the rich information present in the Sentinel-2 satellite data, automatically extracting relevant features and capturing intricate relationships and dependencies that may not be easily captured by the other two deep learning pixel-based classification models. The lower performance of the DeepLab and Pyramid Scene Parsing (PSP) models compared to the UNet model can be attributed to several factors. Firstly, the higher complexity and computational demands of DeepLab, with its atrous convolution, and PSPNet, with its pyramid pooling module, posed significant challenges in fine-tuning hyperparameters, which led to suboptimal performance. Secondly, the complexity of these models requires careful calibration of hyperparameters, and the increased computational load can strain resources, making it difficult to achieve optimal training conditions. The outcomes of our study suggest that the UNet model, with its simpler architecture and fewer computational requirements, is better suited for the task of predicting planted forests across the Republic of Korea. The UNet model's notable performance, particularly in recall (64%), highlights its potential as a reliable tool for forest monitoring and management in this region. This is particularly significant as our objective is to maximize the identification of these areas. Leveraging specific data sources used for its training, the UNet model provides improved predictions and demonstrates robustness in handling the varied ecoregions of the Korean Peninsula. This performance makes the model a valuable asset for forest monitoring and management efforts, offering improved reliable predictions and a practical balance between complexity and computational efficiency.

However, while the UNet model has shown promising results, there remains room for further enhancement to optimize its performance. Comparative analysis with the RF machine learning model reveals nuanced differences. Despite similar F1 values, the UNet model stands out with a more balanced precision and recall, making it well-suited for achieving more equitable predictions. In contrast, the RF model exhibits a high precision (92%), whereas the recall of the RF model is lower (55.2%). This indicates that although most of the areas identified as planted forests by the RF model turned out to be true, the RF model missed capturing 44.8% of actual planted forest areas. The result thus highlights their respective strengths and weaknesses in the context of identifying planted forests. Firstly, in terms of accuracy metrics specifically recall, the UNet model demonstrated superior efficacy in maximizing the identification of all planted areas. Conversely, the RF model excelled in minimizing false positives, rendering it more reliable in certain contexts. Secondly, regarding data dependency, the UNet model relied exclusively on remote sensing imagery, providing a straightforward approach to data analysis. In contrast, the RF model's reliance on heterogeneous datasets led to decreased recall performance due to complexities in data preprocessing. In spatial pattern capture, UNet outperformed RF due to its specialized architecture and advanced learning capabilities tailored for image

segmentation tasks. The unique design of UNet enabled effective representation of both local and global spatial patterns, complemented by data augmentation techniques for enhanced generalization. While the RF model captures spatial patterns to some extent, UNet's specialized architecture and learning mechanisms make it more proficient in precise spatial pattern detection, particularly in image segmentation applications. Thirdly, concerning computational efficiency, the deep learning model demanded significantly more time and resources due to its utilization of high-resolution satellite imagery inputs, as opposed to the RF model. It is therefore recommended to choose between the UNet and RF models for planted forest identification based on a thorough consideration of the trade-offs between precision and recall, the specific dataset available, and the computational resources and time constraints. However, it is crucial to acknowledge certain limitations of our study, including the availability and quality of the training data, and the applicability of the model to other regions or time periods. As the field of deep learning continues to evolve, incorporating Supplementary Data sources and refining training protocols could potentially yield further enhancements to the UNet model's predictive power. These refinements could lead to even more precise and dependable predictions for a broader range of forest monitoring and management applications. Thin and transparent clouds, containing ground target reflectance information [46], may be addressed in data augmentation. It is therefore essential to conduct a more advanced analysis to simulate the reflectance of ground targets under very thin cloud cover.

In this study, we demonstrated that the UNet deep learning algorithm holds significant promise in the field of remote sensing for forestry applications. Our current methodology has shown considerable adaptability across different ecoregions, illustrating its versatility within varied ecological conditions. For instance, we successfully mapped the coastal regions of Jeju Island (Southern Korea evergreen forests) and the mountainous areas (Central Korean deciduous forests and Southern Korea evergreen forests) based on the WWF Terrestrial Ecoregions classification [112]. The findings highlight the method's capability to capture diverse ecological characteristics. The integration of Sentinel-2 imagery and the UNet deep learning model effectively identified and mapped planted forests across these distinct ecoregions, highlighting the flexibility of our approach. This suggests that similar frameworks could be applied globally to other ecoregions, enhancing the relevance and applicability of our findings to various ecological contexts. By leveraging advanced deep learning methodologies and high-resolution satellite imagery, we have established a robust framework for mapping and analyzing planted forests on a global scale. Our approach, utilizing technologies such as UNet and Sentinel-2 imagery, therefore offers significant benefits for forest managers, policymakers, and researchers. These methodologies can be adapted to different geographical areas, providing valuable tools for global environmental monitoring and resource management efforts. This study can enhance the accuracy and reliability of forest mapping, making significant contributions to remote sensing, ecological research, and practical forestry applications. By showcasing the effectiveness of these technologies, we advocate for their broader adoption in various environmental and resource management initiatives.

5. Conclusions

This research thus has a broad scope, aiming to enhance our understanding of the benefits and lessons learned from Korea's massive tree plantation projects. By examining previous reforestation projects in Korea and other countries, this study can inform ongoing and future reforestation projects worldwide, enabling stakeholders to maximize the ecological and socioeconomic benefits of planted forests. This study is particularly timely given that many countries, including the United States, have joined the World Economic Forum's One Trillion Trees Initiative, an ambitious global effort to grow and conserve one trillion trees worldwide by 2030. By leveraging big data and artificial intelligence tools, the findings from this study can help us better restore the forests based on past experiences, bringing us one step closer to sustainable forest management and mitigating climate change

through increased terrestrial carbon sequestration from planted forests. The framework developed through this research therefore demonstrates the versatility and scalability of integrating advanced remote sensing and deep learning techniques for environmental monitoring across various ecosystems and geographic regions. This synergistic approach enhances the accuracy of forest mapping and provides a robust system for continuous monitoring and adaptive management of forest resources. By advancing technical capabilities and deepening our understanding of reforestation dynamics, this study significantly contributes to global efforts in addressing complex environmental challenges and fostering sustainable development.

Supplementary Materials: The following supporting information can be downloaded at <https://www.mdpi.com/article/10.3390/f15071216/s1>, Box S1: Outline of Models Used with associated Bibliography.

Author Contributions: J.L. and N.L.H. conceived the study; A.M. and C.I.A. coordinated data compilation; A.M. conducted data analysis and wrote the initial draft; J.L. supervised the manuscript development; everyone contributed to the writing, revision, and editing. All authors have read and agreed to the published version of the manuscript.

Funding: This study is supported, in parts, by the World Resources Institute (WRI) project “Mapping planted forests in China”, and by the Department of Forestry and Natural Resources, Purdue University. We thank the Global Forest Biodiversity Initiative (GFBI) and Science-i (Project#EA-2024-001) for facilitating data sharing and international research collaboration.

Data Availability Statement: Analyzed data can be provided upon request. To ensure the reproducibility of our study, we have made the deep learning semantic segmentation models used in our research available on our GitHub repository (<https://github.com/mitrankita92/Semantic-segmentation> (accessed on 28 May 2024)). The codebase includes all the necessary scripts and configuration files required to run the model and reproduce the results reported in our manuscript. By making the code available in publicly accessible repositories, we aim to promote transparency, reproducibility, and scientific integrity. We believe that providing access to these resources will enable other researchers to validate our findings, replicate our experiments, and build upon our work to advance the field of semantic segmentation in remote sensing and related areas.

Acknowledgments: We would like to express our sincere gratitude to the Global Forest Biodiversity Initiative (GFBI) and Science-i for their valuable assistance in data sharing and promoting international research collaboration. We would also like to acknowledge the use of super-computer facilities at Purdue University for data analysis, which greatly contributed to the completion of this research.

Conflicts of Interest: The authors declare no conflicts of interest.

References

1. FAO. *Global Forest Resources Assessment 2020: Main Report*; Food and Agriculture Organization of the United Nations: Rome, Italy, 2020.
2. Law, B.E.; Hudiburg, T.W.; Berner, L.T.; Kent, J.J.; Buotte, P.C.; Harmon, M.E. Land Use Strategies to Mitigate Climate Change in Carbon Dense Temperate Forests. *Proc. Natl. Acad. Sci. USA* **2018**, *115*, 3663–3668. [[CrossRef](#)] [[PubMed](#)]
3. Moomaw, W.R.; Law, B.E.; Goetz, S.J. Focus on the Role of Forests and Soils in Meeting Climate Change Mitigation Goals: Summary. *Environ. Res. Lett.* **2020**, *15*, 045009. [[CrossRef](#)]
4. Nunes, L.J.; Meireles, C.I.; Pinto Gomes, C.J.; Almeida Ribeiro, N.M. Forest Contribution to Climate Change Mitigation: Management Oriented to Carbon Capture and Storage. *Climate* **2020**, *8*, 21. [[CrossRef](#)]
5. Potapov, P.; Hansen, M.C.; Pickens, A.; Hernandez-Serna, A.; Tyukavina, A.; Turubanova, S.; Zalles, V.; Li, X.; Khan, A.; Stolle, F.; et al. The Global 2000–2020 Land Cover and Land Use Change Dataset Derived from the Landsat Archive: First Results. *Front. Remote Sens.* **2022**, *3*, 856903. [[CrossRef](#)]
6. Abdollahnejad, A.; Panagiotidis, D. Tree Species Classification and Health Status Assessment for a Mixed Broadleaf-Conifer Forest with UAS Multispectral Imaging. *Remote Sens.* **2020**, *12*, 3722. [[CrossRef](#)]
7. Senf, C.; Seidl, R.; Hostert, P. Remote Sensing of Forest Insect Disturbances: Current State and Future Directions. *Int. J. Appl. Earth Obs. Geoinf.* **2017**, *60*, 49–60. [[CrossRef](#)] [[PubMed](#)]
8. Housman, I.W.; Chastain, R.A.; Finco, M.V. An Evaluation of Forest Health Insect and Disease Survey Data and Satellite-Based Remote Sensing Forest Change Detection Methods: Case Studies in the United States. *Remote Sens.* **2018**, *10*, 1184. [[CrossRef](#)]
9. Torres, P.; Rodes-Blanco, M.; Viana-Soto, A.; Nieto, H.; García, M. The Role of Remote Sensing for the Assessment and Monitoring of Forest Health: A Systematic Evidence Synthesis. *Forests* **2021**, *12*, 1134. [[CrossRef](#)]

10. Lausch, A.; Erasmí, S.; King, D.J.; Magdon, P.; Heurich, M. Understanding Forest Health with Remote Sensing—Part I: A Review of Spectral Traits, Processes and Remote-Sensing Characteristics. *Remote Sens.* **2016**, *8*, 1029. [[CrossRef](#)]
11. Stone, C.; Mohammed, C. Application of Remote Sensing Technologies for Assessing Planted Forests Damaged by Insect Pests and Fungal Pathogens: A Review. *Curr. For. Rep.* **2017**, *3*, 75–92. [[CrossRef](#)]
12. Brancalion, P.H.S.; Holl, K.D. Guidance for Successful Tree Planting Initiatives. *J. Appl. Ecol.* **2020**, *57*, 2349–2361. [[CrossRef](#)]
13. Abbasi, A.O.; Tang, X.; Harris, N.L.; Goldman, E.D.; Gamarra, J.G.P.; Herold, M.; Kim, H.S.; Luo, W.; Silva, C.A.; Tchebakova, N.M.; et al. Spatial Database of Planted Forests in East Asia. *Sci. Data* **2023**, *10*, 480. [[CrossRef](#)] [[PubMed](#)]
14. Lesiv, M.; Schepaschenko, D.; Buchhorn, M.; See, L.; Duerauer, M.; Georgieva, I.; Jung, M.; Hofhansl, F.; Schulze, K.; Bilous, A.; et al. *Global Planted Trees Extent 2015*; Zenodo: Geneva, Switzerland, 2020. [[CrossRef](#)]
15. Paquette, A.; Messier, C. The Role of Plantations in Managing the World’s Forests in the Anthropocene. *Front. Ecol. Environ.* **2010**, *8*, 27–34. [[CrossRef](#)]
16. Lee, D.; Lee, Y. Roles of Saemaul Undong in Reforestation and NGO Activities for Sustainable Forest Management in Korea. *J. Sustain. For.* **2005**, *20*, 1–16. [[CrossRef](#)]
17. Park, M.S.; Youn, Y.-C. Reforestation Policy Integration by Multiple Sectors Toward Forest Transition in the Republic of Korea. *For. Policy Econ.* **2017**, *76*, 45–55. [[CrossRef](#)]
18. Evans, D.S.; Schmalensee, R. *The Industrial Organization of Markets with Two-Sided Platforms*; Working Paper No. 11603; National Bureau of Economic Research: Cambridge, MA, USA, 2005. [[CrossRef](#)]
19. Koch, R.; Almeida-Cortez, J.S.; Kleinschmit, B. Revealing Areas of High Nature Conservation Importance in a Seasonally Dry Tropical Forest in Brazil: Combination of Modelled Plant Diversity Hot Spots and Threat Patterns. *J. Nat. Conserv.* **2017**, *35*, 24–39. [[CrossRef](#)]
20. Harris, N.; Goldman, E.D.; Gibbes, S. *Spatial Database of Planted Trees (SDPT Version 1.0)*; Technical Note; World Resources Institute: Washington, DC, USA, 2019.
21. Chen, Y.; Li, Y.; Wang, J.; Chen, W.; Zhang, X. Remote Sensing Image Ship Detection under Complex Sea Conditions Based on Deep Semantic Segmentation. *Remote Sens.* **2020**, *12*, 625. [[CrossRef](#)]
22. Kemker, R.; Salvaggio, C.; Kanan, C. Algorithms for Semantic Segmentation of Multispectral Remote Sensing Imagery Using Deep Learning. *ISPRS J. Photogramm. Remote Sens.* **2018**, *145*, 60–77. [[CrossRef](#)]
23. Yuan, X.; Shi, J.; Gu, L. A Review of Deep Learning Methods for Semantic Segmentation of Remote Sensing Imagery. *Expert Syst. Appl.* **2021**, *169*, 114417. [[CrossRef](#)]
24. Martins, J.A.C.; Nogueira, K.; Osco, L.P.; Gomes, F.D.G.; Furuya, D.E.G.; Gonçalves, W.N.; Junior, J.M. Semantic Segmentation of Tree-Canopy in Urban Environment with Pixel-Wise Deep Learning. *Remote Sens.* **2021**, *13*, 3054. [[CrossRef](#)]
25. Bragagnolo, L.; da Silva, R.V.; Grzybowski, J.M.V. Amazon Forest Cover Change Mapping Based on Semantic Segmentation by U-Nets. *Ecol. Inform.* **2021**, *62*, 101279. [[CrossRef](#)]
26. Sothe, C.; La Rosa, L.E.C.; De Almeida, C.M.; Gonsamo, A.; Schimalski, M.B.; Castro, J.D.B.; Tommaselli, A.M.G. Evaluating a Convolutional Neural Network for Feature Extraction and Tree Species Classification Using UAV-Hyperspectral Images. *ISPRS Ann. Photogramm. Remote Sens. Spat. Inf. Sci.* **2020**, *3*, 193–199. [[CrossRef](#)]
27. Egli, S.; Höpke, M. CNN-Based Tree Species Classification Using High Resolution RGB Image Data from Automated UAV Observations. *Remote Sens.* **2020**, *12*, 3892. [[CrossRef](#)]
28. Li, H.; Hu, B.; Li, Q.; Jing, L. CNN-Based Individual Tree Species Classification Using High-Resolution Satellite Imagery and Airborne LiDAR Data. *Forests* **2021**, *12*, 1697. [[CrossRef](#)]
29. Campos-Taberner, M.; García-Haro, F.J.; Martínez, B.; Sánchez-Ruiz, S.; Gilabert, M.A. A Copernicus Sentinel-1 and Sentinel-2 Classification Framework for the 2020+ European Common Agricultural Policy: A Case Study in València (Spain). *Agronomy* **2019**, *9*, 556. [[CrossRef](#)]
30. Simón Sánchez, A.M.; González-Piqueras, J.; de la Ossa, L.; Calera, A. Convolutional Neural Networks for Agricultural Land Use Classification from Sentinel-2 Image Time Series. *Remote Sens.* **2022**, *14*, 5373. [[CrossRef](#)]
31. Nunes, L.; Moreno, M.; Alberdi, I.; Álvarez-González, J.G.; Godinho-Ferreira, P.; Mazzoleni, S.; Castro Rego, F. Harmonized Classification of Forest Types in the Iberian Peninsula Based on National Forest Inventories. *Forests* **2020**, *11*, 1170. [[CrossRef](#)]
32. Huechacona-Ruiz, A.H.; Dupuy, J.M.; Schwartz, N.B.; Powers, J.S.; Reyes-García, C.; Tun-Dzul, F.; Hernández-Stefanoni, J.L. Mapping Tree Species Deciduousness of Tropical Dry Forests Combining Reflectance, Spectral Unmixing, and Texture Data from High-Resolution Imagery. *Forests* **2020**, *11*, 1234. [[CrossRef](#)]
33. Holzinger, A.; Keiblinger, K.; Holub, P.; Zatloukal, K.; Müller, H. AI for Life: Trends in Artificial Intelligence for Biotechnology. *New Biotechnol.* **2023**, *74*, 16–24. [[CrossRef](#)]
34. Liu, L.; Wang, J.; Zhang, E.; Li, B.; Zhu, X.; Zhang, Y.; Peng, J. Shallow-Deep Convolutional Network and Spectral-Discrimination-Based Detail Injection for Multispectral Imagery Pan-Sharpener. *IEEE J. Sel. Top. Appl. Earth Obs. Remote Sens.* **2020**, *13*, 1772–1783. [[CrossRef](#)]
35. Liu, X.; Faes, L.; Kale, A.U.; Wagner, S.K.; Fu, D.J.; Bruynseels, A.; Mahendiran, T.; Moraes, G.; Shamdass, M.; Kern, C.; et al. A Comparison of Deep Learning Performance Against Health-Care Professionals in Detecting Diseases from Medical Imaging: A Systematic Review and Meta-Analysis. *Lancet Digital Health* **2019**, *1*, e271–e297. [[CrossRef](#)]
36. Du, G.; Cao, X.; Liang, J.; Chen, X.; Zhan, Y. Medical Image Segmentation Based on U-Net: A Review. *J. Imaging Sci. Technol.* **2020**, *64*, 2. [[CrossRef](#)]

37. Wessel, J.; Heinrich, M.P.; von Berg, J.; Franz, A.; Saalbach, A. Sequential Rib Labeling and Segmentation in Chest X-ray Using Mask R-CNN. *arXiv* **2019**, arXiv:1908.08329.
38. Livne, M.; Rieger, J.; Aydin, O.U.; Taha, A.A.; Akay, E.M.; Kossen, T.; Madai, V.I. A U-Net Deep Learning Framework for High Performance Vessel Segmentation in Patients with Cerebrovascular Disease. *Front. Neurosci.* **2019**, *13*, 97. [[CrossRef](#)]
39. Pouliot, D.; Latifovic, R.; Olthof, I.; Fraser, R.; Chen, W. Improved Mapping of Canada's Forest Change with Updated Pixel-Based and Object-Based Methods, 1985–2015. *Can. J. Remote Sens.* **2021**, *47*, 1–19.
40. Fuller, D.O. Tropical Forest Monitoring and Remote Sensing: A New Era of Transparency in Forest Governance? *Singap. J. Trop. Geogr.* **2006**, *27*, 15–29. [[CrossRef](#)]
41. Zhang, T.; Su, J.; Xu, Z.; Luo, Y.; Li, J. Sentinel-2 Satellite Imagery for Urban Land Cover Classification by Optimized Random Forest Classifier. *Appl. Sci.* **2021**, *11*, 543. [[CrossRef](#)]
42. Abdi, A.M. Land Cover and Land Use Classification Performance of Machine Learning Algorithms in a Boreal Landscape Using Sentinel-2 Data. *GISci. Remote Sens.* **2020**, *57*, 1–20.
43. Xi, Y.; Tian, J.; Jiang, H.; Tian, Q.; Xiang, H.; Xu, N. Mapping Tree Species in Natural and Planted Forests Using Sentinel-2 Images. *Remote Sens. Lett.* **2022**, *13*, 544–555. [[CrossRef](#)]
44. Ma, M.; Liu, J.; Liu, M.; Zeng, J.; Li, Y. Tree Species Classification Based on Sentinel-2 Imagery and Random Forest Classifier in the Eastern Regions of the Qilian Mountains. *Forests* **2021**, *12*, 1736. [[CrossRef](#)]
45. Belgiu, M.; Drăguț, L. Random Forest in Remote Sensing: A Review of Applications and Future Directions. *ISPRS J. Photogramm. Remote Sens.* **2016**, *114*, 24–31. [[CrossRef](#)]
46. Bai, Y.; Yang, K.; Mei, T.; Ma, W.-Y.; Zhao, T. Automatic Data Augmentation from Massive Web Images for Deep Visual Recognition. *ACM Trans. Multimed. Comput. Commun. Appl.* **2018**, *14*, 69. [[CrossRef](#)]
47. Nti, I.K.; Nyarko-Boateng, O.; Aning, J. Performance of machine learning algorithms with different K values in K-fold Cross Validation. *Int. J. Inf. Technol. Comput. Sci.* **2021**, *13*, 61–71. [[CrossRef](#)]
48. Kim, J.; Choi, H.; Shin, W.; Yun, J.; Song, Y. *Complex Spatiotemporal Changes in Land-Use and Ecosystem Services in the Jeju Island UNESCO Heritage and Biosphere Site (Republic of Korea)*; Published Online by Cambridge University Press: Cambridge, UK, 2022.
49. Kim, K.; Park, O.J.; Barr, J.; Yun, H.J. Tourists' Shifting Perceptions of UNESCO Heritage Sites: Lessons from Jeju Island—South Korea. *Tour. Rev.* **2019**, *74*, 20–29. [[CrossRef](#)]
50. Hong, H.J.; Kim, C.K.; Lee, H.W.; Lee, W.K. Conservation, Restoration, and Sustainable Use of Biodiversity Based on Habitat Quality Monitoring: A Case Study on Jeju Island, South Korea (1989–2019). *Land* **2021**, *10*, 774. [[CrossRef](#)]
51. Available online: https://developers.google.com/earth-engine/datasets/catalog/COPERNICUS_S2_SR_HARMONIZED (accessed on 30 January 2022).
52. Google Earth Engine: Planetary-Scale geospatial analysis for everyone. *Remote Sens. Environ.* **2017**, *202*, 18–27. [[CrossRef](#)]
53. Liu, H.; Jezek, K.C.; O'Kelly, M.E. Detecting Outliers in Irregularly Distributed Spatial Data Sets by Locally Adaptive and Robust Statistical Analysis and GIS. *Int. J. Geogr. Inf. Sci.* **2001**, *15*, 721–741. [[CrossRef](#)]
54. López-Puigdollers, D.; Mateo-García, G.; Gómez-Chova, L. Benchmarking Deep Learning Models for Cloud Detection in Landsat-8 and Sentinel-2 Images. *Remote Sens.* **2021**, *13*, 992. [[CrossRef](#)]
55. Aybar, C.; Ysuhaylas, L.; Loja, J.; Gonzales, K.; Herrera, F.; Bautista, L.; Gómez-Chova, L. CloudSEN12, a Global Dataset for Semantic Understanding of Cloud and Cloud Shadow in Sentinel-2. *Sci. Data* **2022**, *9*, 782. [[CrossRef](#)] [[PubMed](#)]
56. Taylor, L.; Nitschke, G. Improving Deep Learning with Generic Data Augmentation. In Proceedings of the IEEE Symposium Series on Computational Intelligence (SSCI), Bengaluru, India, 18–21 November 2018; pp. 1542–1547.
57. Mikołajczyk, A.; Grochowski, M. Data Augmentation for Improving Deep Learning in Image Classification Problem. In Proceedings of the International Interdisciplinary PhD Workshop (IIPhDW), Swinoujscie, Poland, 9–12 May 2018; pp. 117–122.
58. Perez, L.; Wang, J. The Effectiveness of Data Augmentation in Image Classification Using Deep Learning. *arXiv* **2017**, arXiv:1712.04621.
59. Ronneberger, O.; Fischer, P.; Brox, T. U-Net: Convolutional Networks for Biomedical Image Segmentation. In Proceedings of the Medical Image Computing and Computer-Assisted Intervention—MICCAI 2015: 18th International Conference, Munich, Germany, 5–9 October 2015; pp. 234–241. [[CrossRef](#)]
60. He, K.; Zhang, X.; Ren, S.; Sun, J. Deep Residual Learning for Image Recognition. In Proceedings of the IEEE Conference on Computer Vision and Pattern Recognition (CVPR), Las Vegas, NV, USA, 27–30 June 2016; pp. 770–778.
61. Smith, L.N. A Disciplined Approach to Neural Network Hyper-Parameters: Part 1—Learning Rate, Batch Size, Momentum, and Weight Decay. *arXiv* **2018**, arXiv:1803.09820.
62. Breiman, L. Random Forests. *Mach. Learn.* **2001**, *45*, 5–32. [[CrossRef](#)]
63. Kocon, K.; Krämer, M.; Würz, H.M. Comparison of CNN-Based Segmentation Models for Forest Type Classification. *AGILE GIScience Ser.* **2022**, *3*, 42. [[CrossRef](#)]
64. LeCun, Y.; Bengio, Y.; Hinton, G. Deep Learning. *Nature* **2015**, *521*, 436–444. [[CrossRef](#)] [[PubMed](#)]
65. Zeiler, M.D.; Fergus, R. Visualizing and Understanding Convolutional Networks. In Proceedings of the Computer Vision—ECCV 2014: 13th European Conference, Zurich, Switzerland, 6–12 September 2014; Proceedings, Part I. Springer International Publishing: Cham, Switzerland, 2014; pp. 818–833.
66. Long, J.; Shelhamer, E.; Darrell, T. Fully Convolutional Networks for Semantic Segmentation. In Proceedings of the IEEE Conference on Computer Vision and Pattern Recognition, Boston, MA, USA, 7–12 June 2015; pp. 3431–3440.

67. Simonyan, K.; Zisserman, A. Very Deep Convolutional Networks for Large-Scale Image Recognition. *arXiv* **2014**, arXiv:1409.1556.
68. Prusak, W.; Skrzypiec, A.; Turlej, T. Comparison of the Performance of Different Neural Network Architectures and Pre-Trained Neural Networks for the Classification of Forest Flora and Fauna. *Int. Multidiscip. Sci. GeoConf. SGEM* **2023**, *23*, 35–40.
69. Centeno, T.B.; Ferreira, C.; Inga, J.G.; Vélez, A.; Huacho, R.; Vidal, O.D.; Tomazello-Filho, M. Cutting Tools to Optimize Classification Parameters of Timber Species with Convolutional Neural Networks. *Rev. Biol. Trop.* **2023**, *71*, 1.
70. Ünal, Z.; Aktaş, H. Classification of Hazelnut Kernels with Deep Learning. *Postharvest Biol. Technol.* **2023**, *197*, 112225. [[CrossRef](#)]
71. Dheeraj, A.; Chand, S. Deep Learning Model for Automated Image Based Plant Disease Classification. In Proceedings of the International Conference on Intelligent Vision and Computing; Springer Nature: Cham, Switzerland, 2022; pp. 21–32.
72. Wang, Y.; Zhang, W.; Gao, R.; Jin, Z.; Wang, X. Recent Advances in the Application of Deep Learning Methods to Forestry. *Wood Sci. Technol.* **2021**, *55*, 1171–1202. [[CrossRef](#)]
73. Chen, L.-C.; Papandreou, G.; Kokkinos, I.; Murphy, K.; Yuille, A.L. DeepLab: Semantic Image Segmentation with Deep Convolutional Nets, Atrous Convolution, and Fully Connected CRFs. *IEEE Trans. Pattern Anal. Mach. Intell.* **2018**, *40*, 834–848. [[CrossRef](#)] [[PubMed](#)]
74. Zhao, H.; Shi, J.; Qi, X.; Wang, X.; Jia, J. Pyramid Scene Parsing Network. In Proceedings of the IEEE Conference on Computer Vision and Pattern Recognition (CVPR), Honolulu, HI, USA, 21–26 July 2017; pp. 2881–2890.
75. Jadon, S. A Survey of Loss Functions for Semantic Segmentation. In Proceedings of the IEEE Conference on Computational Intelligence in Bioinformatics and Computational Biology (CIBCB), New York, NY, USA, 27–29 October 2020; pp. 1–7.
76. Tiwari, T.; Saraswat, M. A New Modified-UNet Deep Learning Model for Semantic Segmentation. *Multimedia Tools Appl.* **2023**, *82*, 3605–3625. [[CrossRef](#)]
77. Gilmer, J.; Ghorbani, B.; Garg, A.; Kudugunta, S.; Neyshabur, B.; Cardoze, D.; Dahl, G.; Nado, Z.; Firat, O. A Loss Curvature Perspective on Training Instability in Deep Learning. *arXiv* **2021**, arXiv:2110.04369. [[CrossRef](#)]
78. Çınar, Z.M.; Nuhu, A.A.; Zeeshan, Q.; Korhan, O.; Asmael, M.; Safaei, B. Machine Learning in Predictive Maintenance towards Sustainable Smart Manufacturing in Industry 4.0. *Sustainability* **2020**, *12*, 8211. [[CrossRef](#)]
79. Chen, T.; He, T.; Benesty, M.; Khotilovich, V.; Tang, Y.; Cho, H.; Chen, K.; Mitchell, R.; Cano, I.; Zhou, T.; et al. xgboost: Extreme Gradient Boosting. R Package Version 1.6.0.1. Available online: <https://CRAN.R-project.org/package=xgboost> (accessed on 20 December 2022).
80. Liang, J.; Gamarra, J.G.P.; Picard, N.; Zhou, M.; Pijanowski, B.; Jacobs, D.F.; Reich, P.B.; Crowther, T.W.; Nabuurs, G.J.; de-Miguel, S.; et al. Co-limitation Towards Lower Latitudes Shapes Global Forest Diversity Gradients. *Nat. Ecol. Evol.* **2022**, *6*, 1423–1437. [[CrossRef](#)] [[PubMed](#)]
81. Liaw, A.; Wiener, M. Classification and Regression by randomForest. *R News* **2002**, *2*, 18–22.
82. Al-Abdaly, N.M.; Al-Taai, S.R.; Imran, H.; Ibrahim, M. Development of Prediction Model of Steel Fiber-Reinforced Concrete Compressive Strength Using Random Forest Algorithm Combined with Hyperparameter Tuning and K-Fold Cross-Validation. *East.-Eur. J. Enterp. Technol.* **2021**, *5*, 59–65. [[CrossRef](#)]
83. Chiang, C.Y.; Barnes, C.; Angelov, P.; Jiang, R. Deep Learning-Based Automated Forest Health Diagnosis from Aerial Images. *IEEE Access* **2020**, *8*, 144064–144076. [[CrossRef](#)]
84. Diez, Y.; Kentsch, S.; Fukuda, M.; Caceres, M.L.L.; Moritake, K.; Cabezas, M. Deep Learning in Forestry Using UAV-Acquired RGB Data: A Practical Review. *Remote Sens.* **2021**, *13*, 2837. [[CrossRef](#)]
85. Shao, G.; Tang, L.; Zhang, H. Introducing Image Classification Efficacies. *IEEE Access* **2021**, *9*, 134809–134816. [[CrossRef](#)]
86. Kulkarni, A.; Chong, D.; Batarseh, F.A. *Data Democracy*, 1st ed.; Academic Press: Cambridge, MA, USA, 2020; Chapter 5.
87. Zhao, F.; Sun, R.; Zhong, L.; Meng, R.; Huang, C.; Zeng, X.; Wang, Z. Monthly Mapping of Forest Harvesting Using Dense Time Series Sentinel-1 SAR Imagery and Deep Learning. *Remote Sens. Environ.* **2022**, *269*, 112822. [[CrossRef](#)]
88. Lesiv, M.; Schepaschenko, D.; Buchhorn, M.; See, L.; Dürauer, M.; Georgieva, I.; Jung, M.; Hofhansl, F.; Schulze, K.; Bilous, A.; et al. Global Forest Management Data for 2015 at a 100 m Resolution. *Sci. Data* **2022**, *9*, 199. [[CrossRef](#)]
89. Hansen, M.C.; Potapov, P.V.; Moore, R.; Hancher, M.; Turubanova, S.A.; Tyukavina, A.; Thau, D.; Stehman, S.V.; Goetz, S.J.; Loveland, T.R.; et al. High-Resolution Global Maps of 21st-Century Forest Cover Change. *Science* **2013**, *342*, 850–853. [[CrossRef](#)] [[PubMed](#)]
90. Boston, T.; Van Dijk, A.; Larraondo, P.R.; Thackway, R. Comparing CNNs and random forests for Landsat image segmentation trained on a large proxy land cover dataset. *Remote Sens.* **2022**, *14*, 3396. [[CrossRef](#)]
91. Li, W.; Liu, H.; Wang, Y.; Li, Z.; Jia, Y.; Gui, G. Deep Learning-Based Classification Methods for Remote Sensing Images in Urban Built-Up Areas. *IEEE Access* **2019**, *7*, 36274–36284. [[CrossRef](#)]
92. Kussul, N.; Lavreniuk, M.; Skakun, S.; Shelestov, A. Deep Learning Classification of Land Cover and Crop Types Using Remote Sensing Data. *IEEE Geosci. Remote Sens. Lett.* **2017**, *14*, 778–783. [[CrossRef](#)]
93. Lyu, B.; Haque, A. Deep Learning Based Tumor Type Classification Using Gene Expression Data. In Proceedings of the ACM International Conference on Bioinformatics, Computational Biology, and Health Informatics, Washington, DC, USA, 29 August–1 September 2018; pp. 89–96. [[CrossRef](#)]
94. Adegun, A.A.; Dombey, J.V.F.; Viriri, S.; Odindi, J. State-of-the-Art Deep Learning Methods for Objects Detection in Remote Sensing Satellite Images. *Sensors* **2023**, *23*, 5849. [[CrossRef](#)]

95. Schiefer, F.; Kattenborn, T.; Frick, A.; Frey, J.; Schall, P.; Koch, B.; Schmidlein, S. Mapping Forest Tree Species in High Resolution UAV-Based RGB-Imagery by Means of Convolutional Neural Networks. *ISPRS J. Photogramm. Remote Sens.* **2020**, *170*, 205–215. [[CrossRef](#)]
96. Santos, A.A.D.; Marcato Junior, J.; Araújo, M.S.; Di Martini, D.R.; Tetila, E.C.; Siqueira, H.L.; Gonçalves, W.N. Assessment of CNN-Based Methods for Individual Tree Detection on Images Captured by RGB Cameras Attached to UAVs. *Sensors* **2019**, *19*, 3595. [[CrossRef](#)] [[PubMed](#)]
97. Korznikov, K.A.; Kislov, D.E.; Altman, J.; Doležal, J.; Vozmishcheva, A.S.; Krestov, P.V. Using U-Net-Like Deep Convolutional Neural Networks for Precise Tree Recognition in Very High Resolution RGB (Red, Green, Blue) Satellite Images. *Forests* **2021**, *12*, 66. [[CrossRef](#)]
98. Sliney, D.H. What Is Light? The Visible Spectrum and Beyond. *Eye* **2016**, *30*, 222–229. [[CrossRef](#)] [[PubMed](#)]
99. Ozyavuz, M.; Bilgili, B.C.; Salici, A. Determination of Vegetation Changes with NDVI Method. *J. Environ. Prot. Ecol.* **2015**, *16*, 264–273.
100. Zhong, Z.; He, B.; Chen, Y.; Yuan, W.; Huang, L.; Guo, L.; Xie, X. Higher Sensitivity of Planted Forests' Productivity Than Natural Forests to Droughts in China. *J. Geophys. Res. Biogeosci.* **2021**, *126*, e2021JG006306. [[CrossRef](#)]
101. Pettorelli, N.; Vik, J.O.; Mysterud, A.; Gaillard, J.M.; Tucker, C.J.; Stenseth, N.C. Using the Satellite-Derived NDVI to Assess Ecological Responses to Environmental Change. *Trends Ecol. Evol.* **2005**, *20*, 503–510. [[CrossRef](#)] [[PubMed](#)]
102. Trisasongko, B.H.; Paull, D. A Review of Remote Sensing Applications in Tropical Forestry with a Particular Emphasis on the Plantation Sector. *Int. J. Remote Sens.* **2018**, *39*, 317–339. [[CrossRef](#)]
103. Sharrow, S.H. Tree Planting Pattern Effects on Forage Production in a Douglas-Fir Agroforest. *Agrofor. Syst.* **1991**, *16*, 167–175. [[CrossRef](#)]
104. Henskens, F.L.; Battaglia, M.; Cherry, M.L.; Beadle, C.L. Physiological Basis of Spacing Effects on Tree Growth and Form in *Eucalyptus globulus*. *Trees* **2001**, *15*, 365–377. [[CrossRef](#)]
105. Dungan, J.; Johnson, L.; Billow, C.; Matson, P.; Mazzurco, J.; Moen, J.; Vanderbilt, V. High Spectral Resolution Reflectance of Douglas Fir Grown Under Different Fertilization Treatments: Experiment Design and Treatment Effects. *Remote Sens. Environ.* **1996**, *55*, 217–228. [[CrossRef](#)]
106. Amiri, M.; Pourghasemi, H.R. Mapping the NDVI and Monitoring of Its Changes Using Google Earth Engine and Sentinel-2 Images. In *Computers in Earth and Environmental Sciences*; Elsevier: Amsterdam, The Netherlands, 2022; pp. 127–136.
107. de Araújo Carvalho, M.; Junior, J.M.; Martins, J.A.C.; Zamboni, P.; Costa, C.S.; Siqueira, H.L.; Gonçalves, W.N. A Deep Learning-Based Mobile Application for Tree Species Mapping in RGB Images. *Int. J. Appl. Earth Obs. Geoinf.* **2022**, *114*, 103045.
108. da Costa, L.B.; de Carvalho, O.L.F.; de Albuquerque, A.O.; Gomes, R.A.T.; Guimarães, R.F.; de Carvalho Júnior, O.A. Deep Semantic Segmentation for Detecting Eucalyptus Planted Forests in the Brazilian Territory Using Sentinel-2 Imagery. *Geocarto Int.* **2022**, *37*, 6538–6550. [[CrossRef](#)]
109. Illarionova, S.; Shadrin, D.; Trekin, A.; Ignatiev, V.; Oseledets, I. Generation of the NIR Spectral Band for Satellite Images with Convolutional Neural Networks. *Sensors* **2021**, *21*, 5646. [[CrossRef](#)] [[PubMed](#)]
110. Giang, T.L.; Dang, K.B.; Le, Q.T.; Nguyen, V.G.; Tong, S.S.; Pham, V.M. U-Net Convolutional Networks for Mining Land Cover Classification Based on High-Resolution UAV Imagery. *IEEE Access* **2020**, *8*, 186257–186273. [[CrossRef](#)]
111. Cao, K.; Zhang, X. An Improved Res-UNet Model for Tree Species Classification Using Airborne High-Resolution Images. *Remote Sens.* **2020**, *12*, 1128. [[CrossRef](#)]
112. Olson, D.M.; Dinerstein, E.; Wikramanayake, E.D.; Burgess, N.D.; Powell, G.V.N.; Underwood, E.C.; D'Amico, J.A.; Itoua, I.; Strand, H.E.; Morrison, J.C.; et al. Terrestrial Ecoregions of the World: A New Map of Life on Earth. *Bioscience* **2001**, *51*, 933–938. [[CrossRef](#)]

Disclaimer/Publisher's Note: The statements, opinions and data contained in all publications are solely those of the individual author(s) and contributor(s) and not of MDPI and/or the editor(s). MDPI and/or the editor(s) disclaim responsibility for any injury to people or property resulting from any ideas, methods, instructions or products referred to in the content.